

Laboratory of Data Acquisition

Matteo Fossati - Michele Fumagalli - Mario Zannoni

Concepts on telescopes and detectors

Goal: to get familiar with some basic concepts behind astronomical instruments

Outline:

- Telescopes (mounting, optical scheme, focii)
- Detectors (CCD)
- Filters
- Grisms

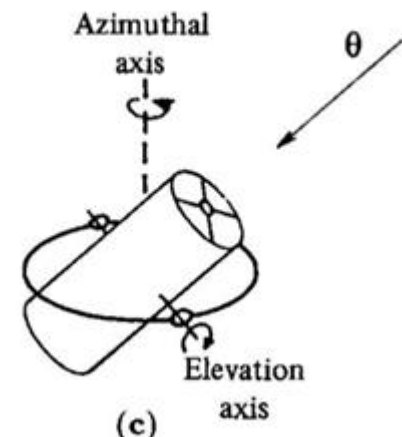
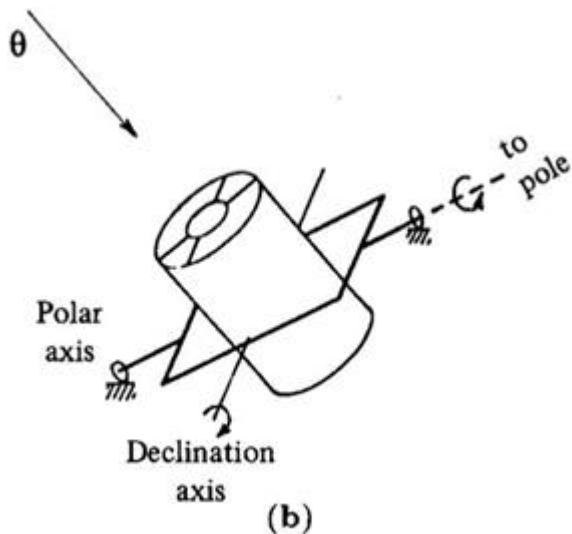
Telescopes mounts: equatorial vs alt-az

Equatorial:

- Simple movement
- Relatively compact
- No de-rotator

Alt-Az:

- Complex movement
- Very compact
- Rotating field of view



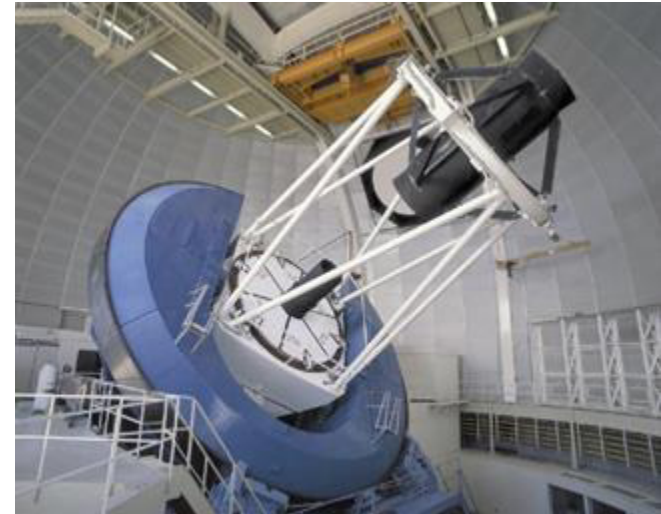
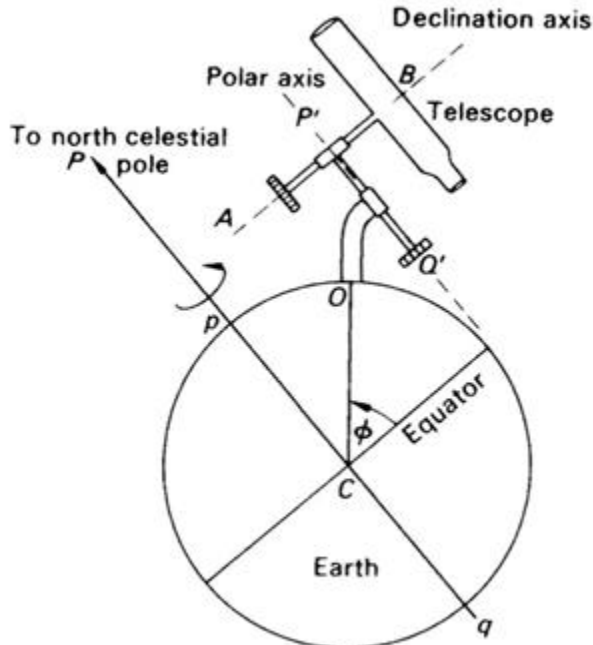
Telescopes mounts: equatorial vs alt-az

Equatorial:

- Simple movement
- Relatively compact
- No de-rotator

Alt-Az:

- Complex movement
- Very compact
- Rotating field of view



Mayall Telescope @ Kitt Peak (4m)

Telescopes mounts: equatorial vs alt-az

All the modern BIG telescopes have Alt-Az mount



Hale @ Mount Palomar (5m Equatorial)



VLT @ Paranal (8.2m)



NTT @ La Silla (3.5m)

Telescopes optics

The most common optical scheme is Ritchey-Chrétien (hyperbolic-hyperbolic)

We skip optical details and keep that it has the *widest* and *most corrected* field of view

Given the telescope aperture D, its resolution is driven by the diffraction limit for a certain wavelength

$$\sin \alpha_n = \frac{m_n \lambda}{D}$$

where m_n is a numerical coefficient

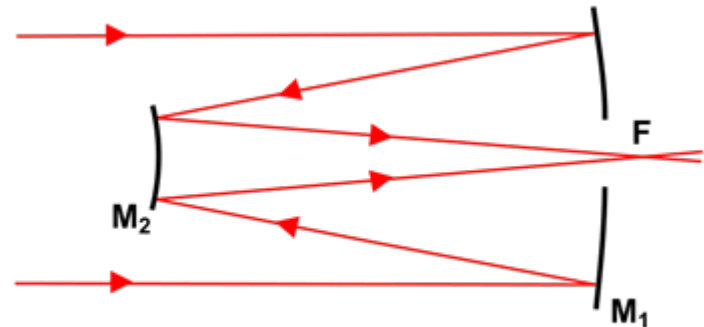
$$\sin \alpha_n \approx \alpha_n$$

$$n=1 \rightarrow m_n=1.22$$

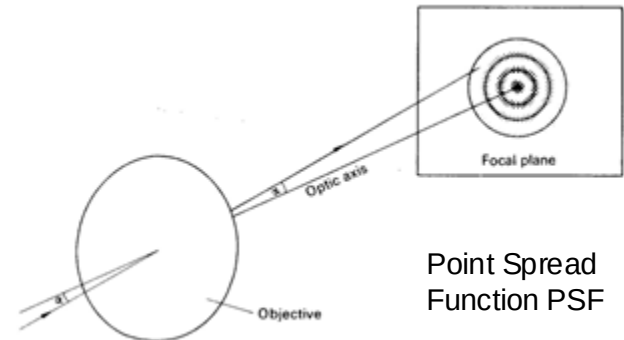
$$\alpha_n = \frac{m_n \lambda}{D}$$

$$n=2 \rightarrow m_n=2.23$$

$$n=3 \rightarrow m_n=3.24$$



Ritchey-Chrétien

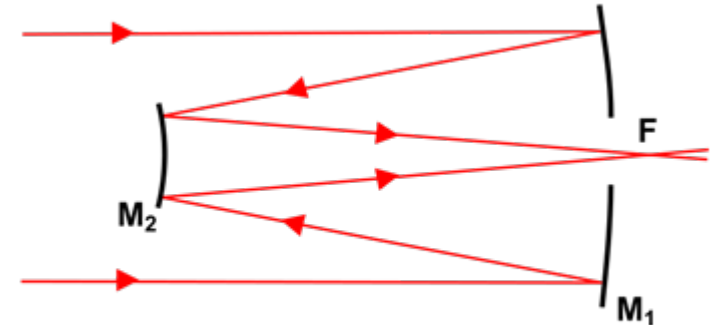


Point Spread
Function PSF

Telescopes optics

The most common optical scheme is Ritchey-Chrétien (hyperbolic-hyperbolic)

We disregard optical details and keep that it has the *widest* and *most corrected* field of view



Ritchey-Chrétien

Given the telescope aperture D, its resolution is driven by the diffraction limit for a certain wavelength

$$\sin \alpha_n = \frac{m_n \lambda}{D}$$

where m_n is a numerical coefficient

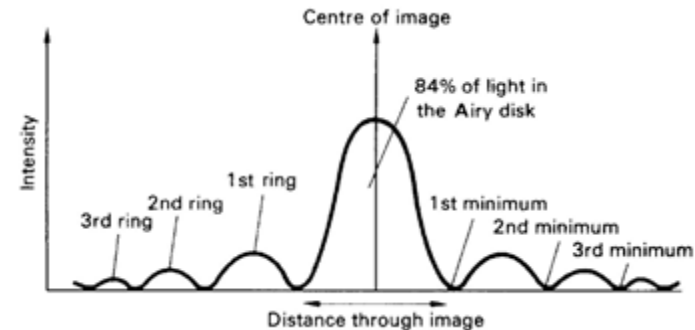
$$\sin \alpha_n \approx \alpha_n$$

$$n=1 \rightarrow m_n=1.22$$

$$\alpha_n = \frac{m_n \lambda}{D}$$

$$n=2 \rightarrow m_n=2.23$$

$$n=3 \rightarrow m_n=3.24$$

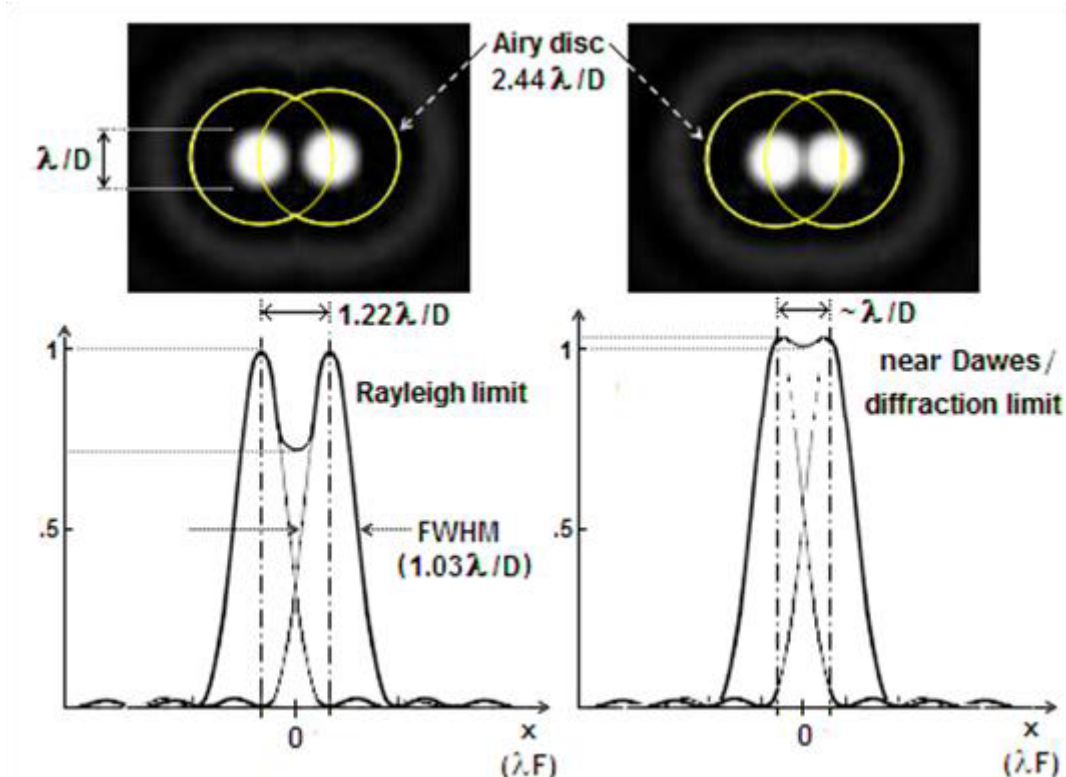


Telescopes optics

Rayleigh Criterium:

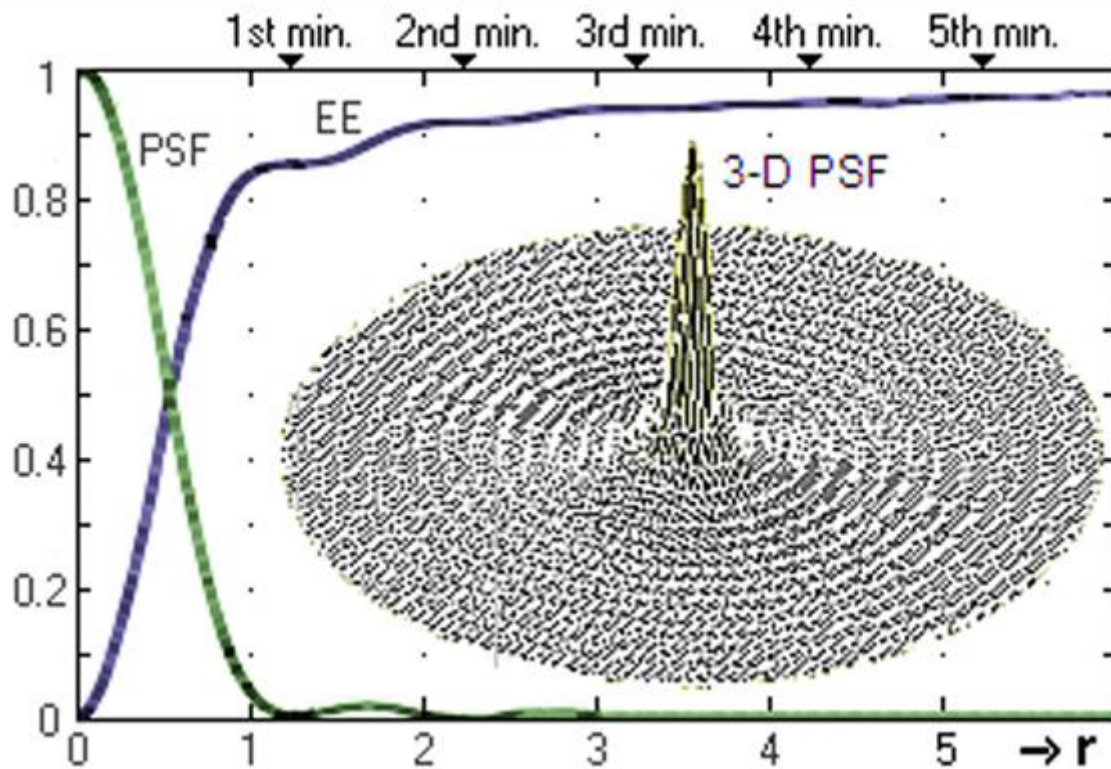
we say that two stars are resolved when the central maximum of the diffraction figure of the first one falls into the first minimum of the second one.

We even call the diffraction figure *point spread function PSF* because represents how a point-like source (a star) is projected (spread) on the focal plane.



Telescopes optics

The Encircled Energy (fundamental for photometry) is directly related to the Point Spread function



Telescopes optics

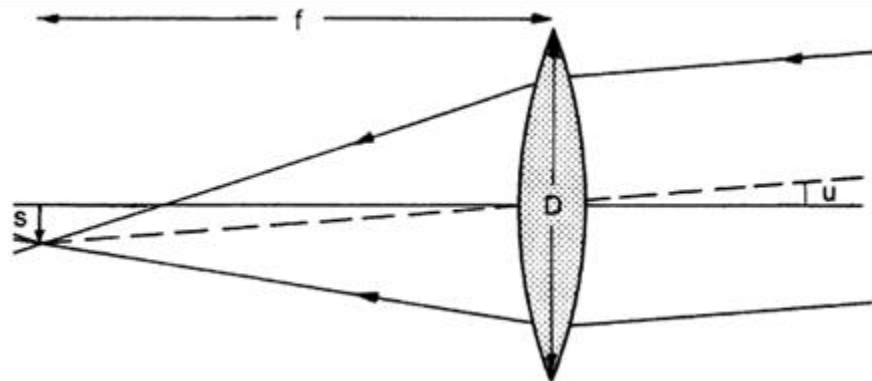
Fotometric Band	λ (nm)	D=2.5 m (HST)	D=3.5 m (NTT)	D=8.2 m (VLT)	D=10.0 m (KECK)
U	365	0.037"	0.026"	0.011"	0.009"
B	440	0.044"	0.032"	0.013"	0.011"
V	550	0.055"	0.039"	0.017"	0.014"
R	700	0.070"	0.050"	0.021"	0.018"
I	900	0.090"	0.065"	0.028"	0.023"
J	1250	0.126"	0.090"	0.038"	0.031"
H	1650	0.166"	0.119"	0.051"	0.041"
K	2200	0.221"	0.158"	0.067"	0.055"
L	3600	0.362"	0.259"	0.110"	0.091"
M	4800	0.483"	0.345"	0.147"	0.121"

Diffraction limits for various famous telescopes.

Only Space Telescope is really diffraction limited because in orbit (no atmosphere, no turbulence, no seeing limit)

Telescopes optics

Plate Scale



$$s = f \cdot \tan u \approx f \cdot u$$

$$\frac{du}{ds} = \frac{1}{f}$$
 PLATE SCALE

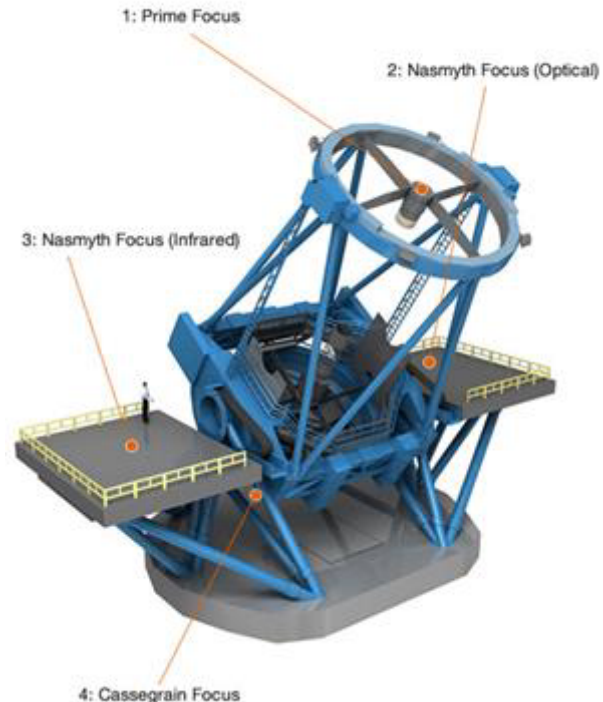
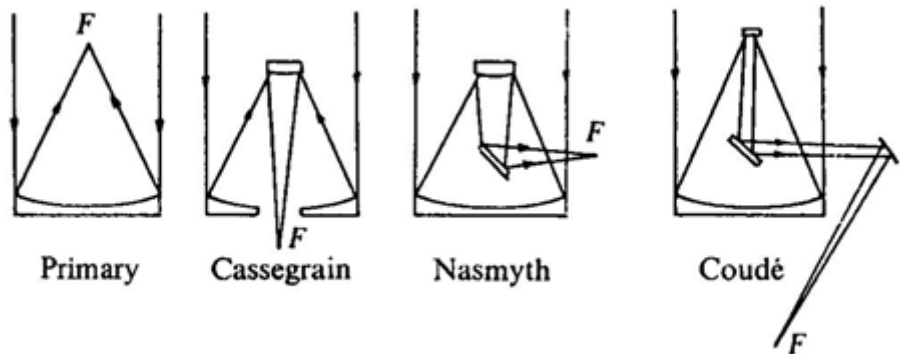
If we call f the focal length of a telescope, the *plate scale* translates the angular separation of two objects into a *physical distance* on the focal plane so that we can know how many arc-sec is a pixel

$$\frac{du}{ds} = \frac{206265(")}{f(mm)}$$

Telescopes optics

A telescope can have many focal stations calle *focii*.

The big instruments are usually hosted at the Nasmyth focii because they are co-axial with the elevation axis

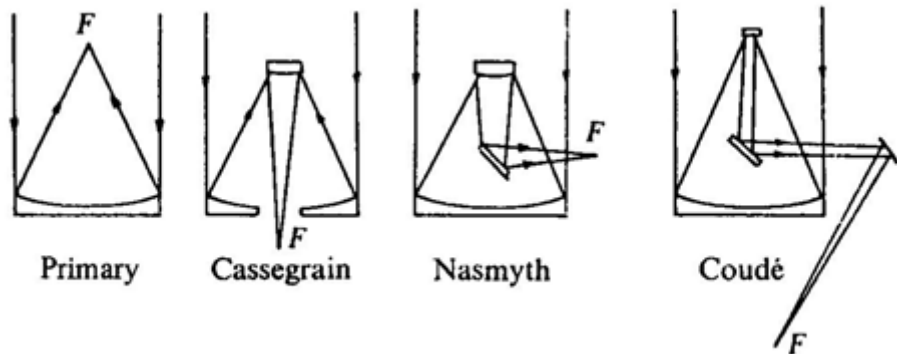


© NAOJ

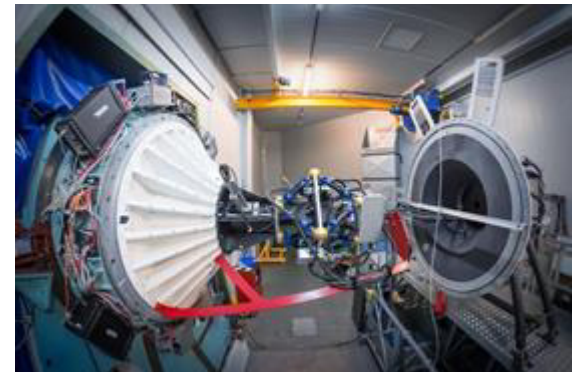
Telescopes optics

A telescope can have many focal stations calle *focii*.

The big instruments are usually hosted at the Nasmyth focii because they are co-axial with the elevation axis



EFOSC2 (top) and ULTRACAM (bottom) @ NTT



TOBi Telescopio Ottico Bicocca



On top of the U9 building

Inside a spherical robotic dome

TOBi Telescopio Ottico Bicocca



Equatorial mount (German type) made by *10micron* company in Italy

Model GM3000 HPS

Weight (mount) 65 kg without accessories

Instrument payload capacity 100 kg

Latitude range 20° – 70°

Azimuth fine adjustment range +/- 10°

Axes R.A. 80 mm diameter, alloy steel, Dec. 50 mm diameter, alloy steel

Transmission system

Backlash-free system with timing belt and automatic backlash recovery

Motors

2 axes servo brushless

Power consumption

~ 1 A while tracking

~ 3.5 A at maximum speed

~ 5 A peak

Go-to-speed Adjustable from 2°/s to 12°/s (9°/s in r.a.)

Pointing accuracy < 20" with internal multiple-stars software mapping

Average tracking accuracy

< +/- 1" typical for 15 minutes (< 0.7" RMS) with multiple-stars software mapping and compensation of flexure and polar alignment errors

TOBi Telescopio Ottico Bicocca

400mm F/7 Modified Ritchey-Chretien telescope By Officina Stellare (Italy)



- We chose a variation on Ritchey-Chretien optical scheme (hyperbolic-hyperbolic) called RiDK (Riccardi-Dall Kirkham)
- a balanced f/7 focal ratio and the 2-lens field flattener
- A plate scale $\frac{d\Theta}{ds} = \frac{206265''}{f(mm)} \sim \frac{74''}{mm}$

TOBi Telescopio Ottico Bicocca

Photometric Camera Atik 16200 mono

- Sensor Type: CCD - KAF-16200 APS cut (35mm diagonal)
- Horizontal Resolution: 4499 pixels
- Vertical Resolution: 3599 pixels
- **Pixel Size: 6 μm x 6 μm**
- ADC: 16 bit
- **Readout Noise: 9e- typical value**
- Gain Factor: 0.6e-/ ADU
- Full Well: ~40,000e-
- **Dark Current: >0.25 electrons/second at 0°C**
- Maximum Exposure Length: Unlimited
- Minimum Exposure Length: 200 ms
- Cooling: Thermoelectric set point with max $\Delta T = >-50^\circ\text{C}$
- **6 μm pixel means 0.44"/pix**

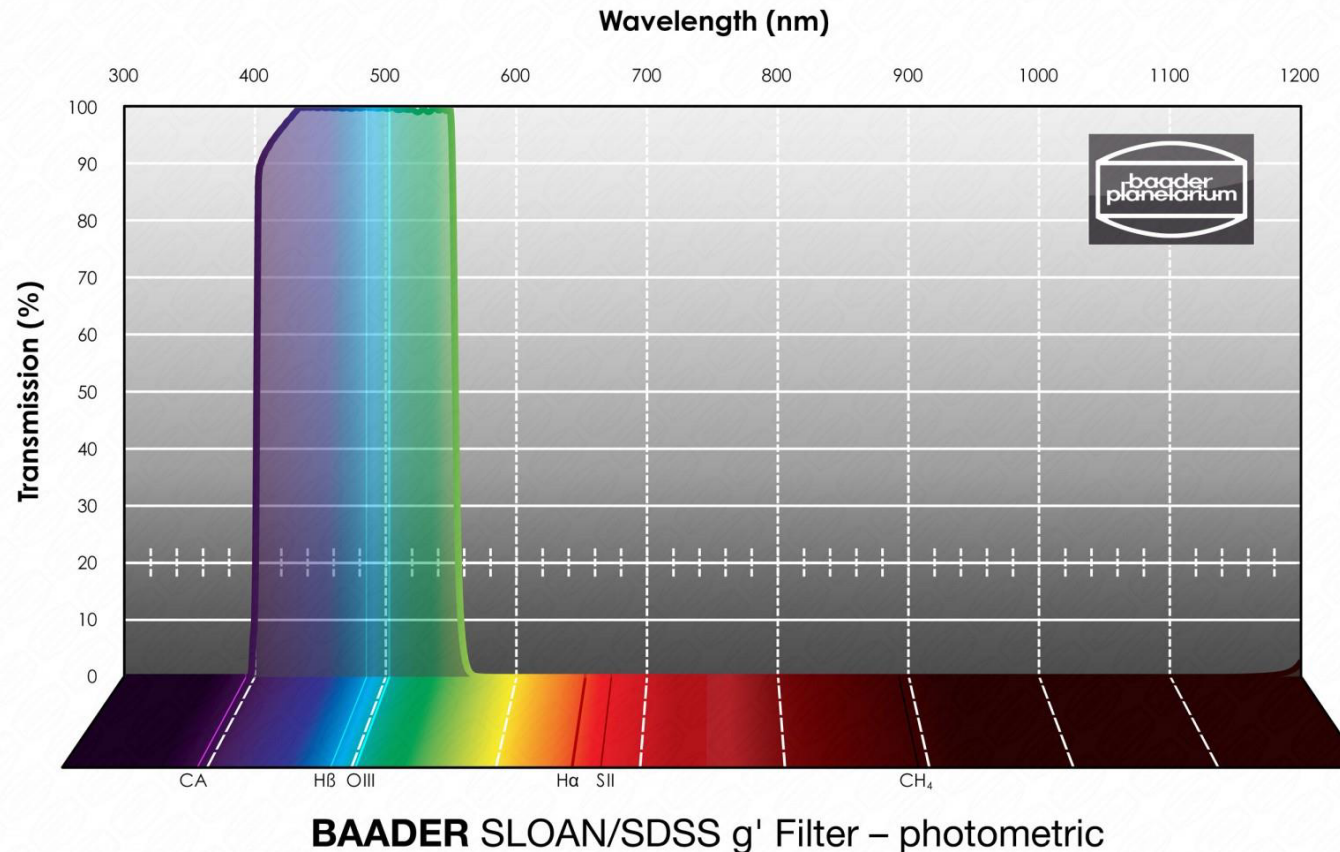


TOBi Telescopio Ottico Bicocca

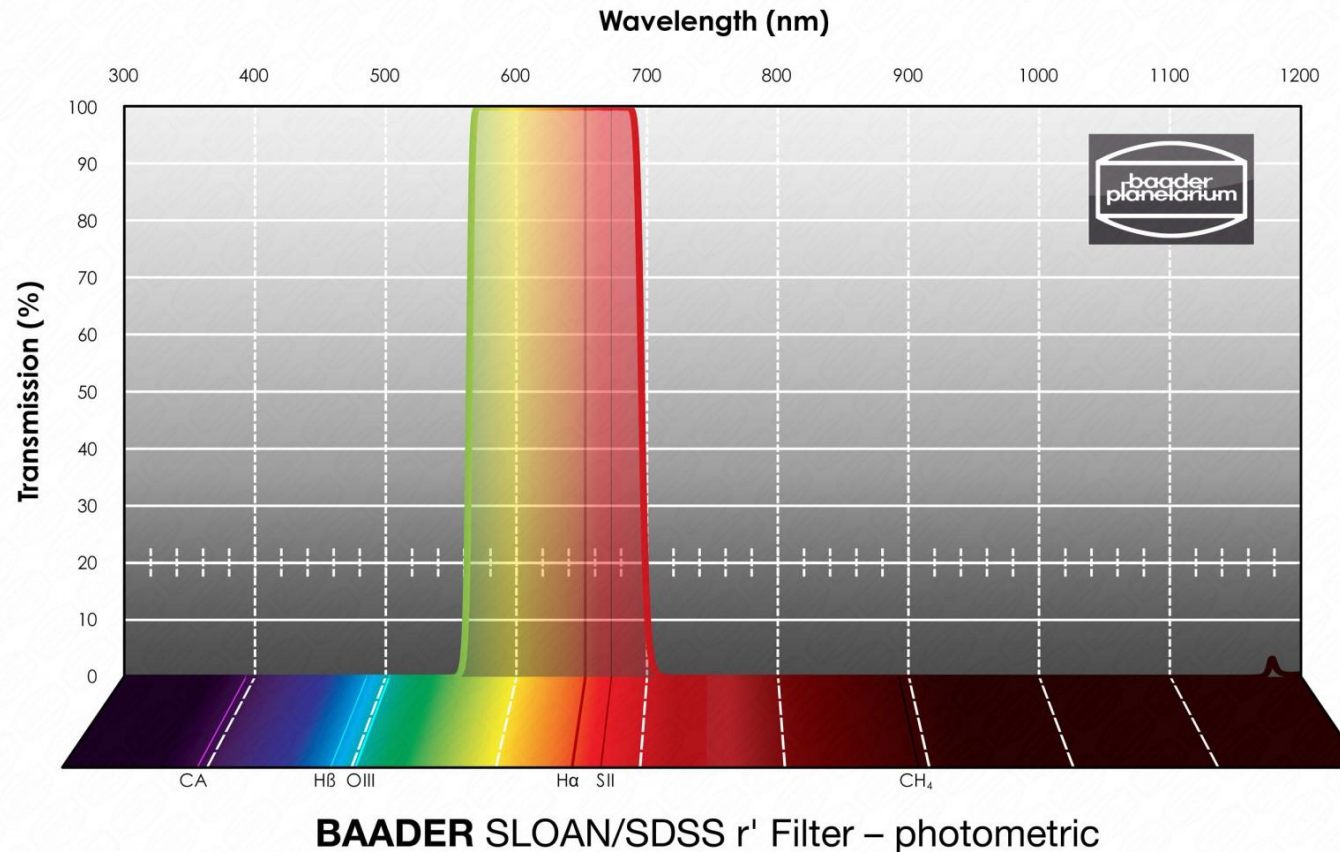
- Photometric Camera
 - Atik 16200 mono
 - 7 positions 2" Filter wheel
 - H- α (656nm, 3.5nm wide)
 - H- β (486nm, 5.5nm wide)
 - OIII (500nm, 4nm wide)
 - SII (672nm, 4nm wide)
 - g' (477nm, ~150nm wide)
 - r' (658nm, ~140nm wide)
 - i' (806nm, ~150nm wide)



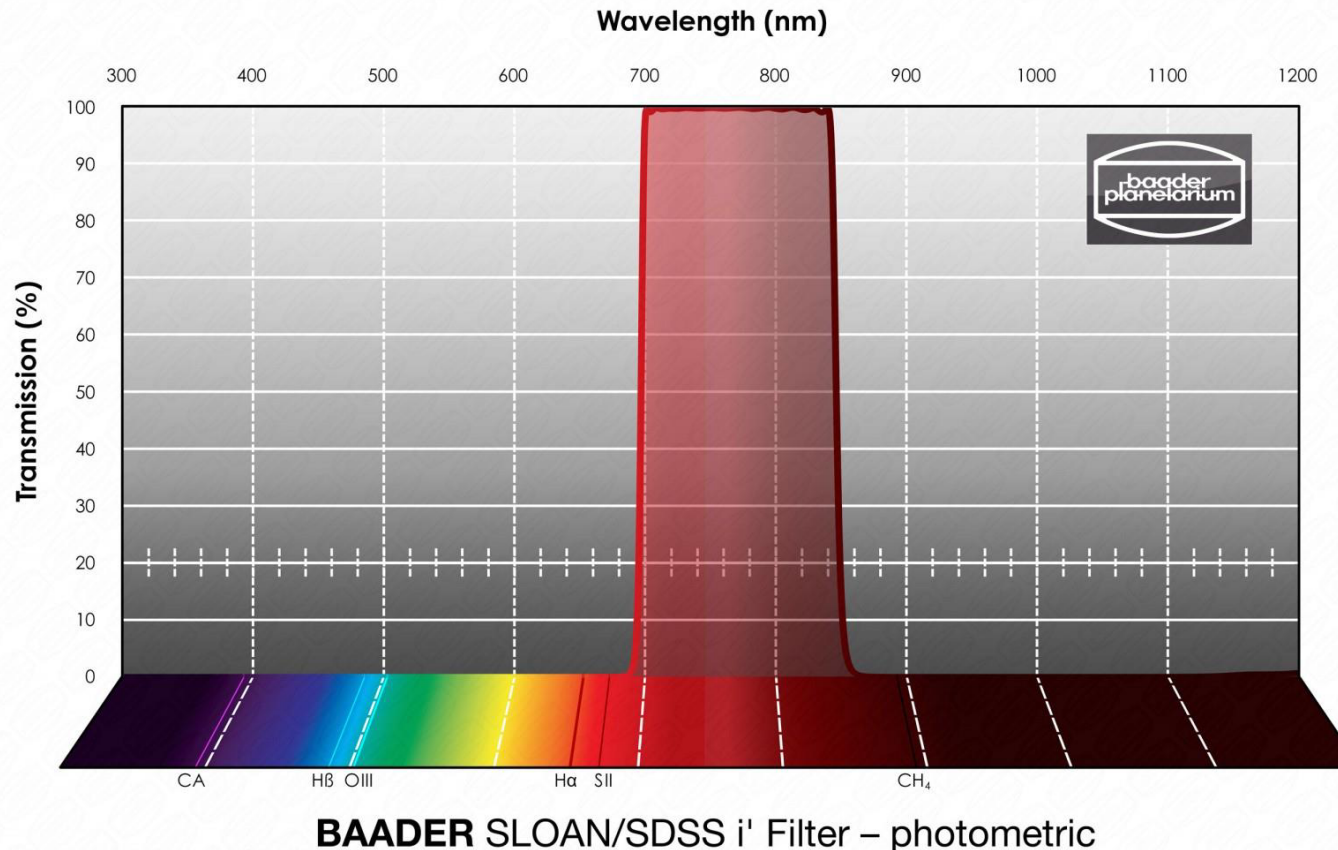
TOBi Telescopio Ottico Bicocca



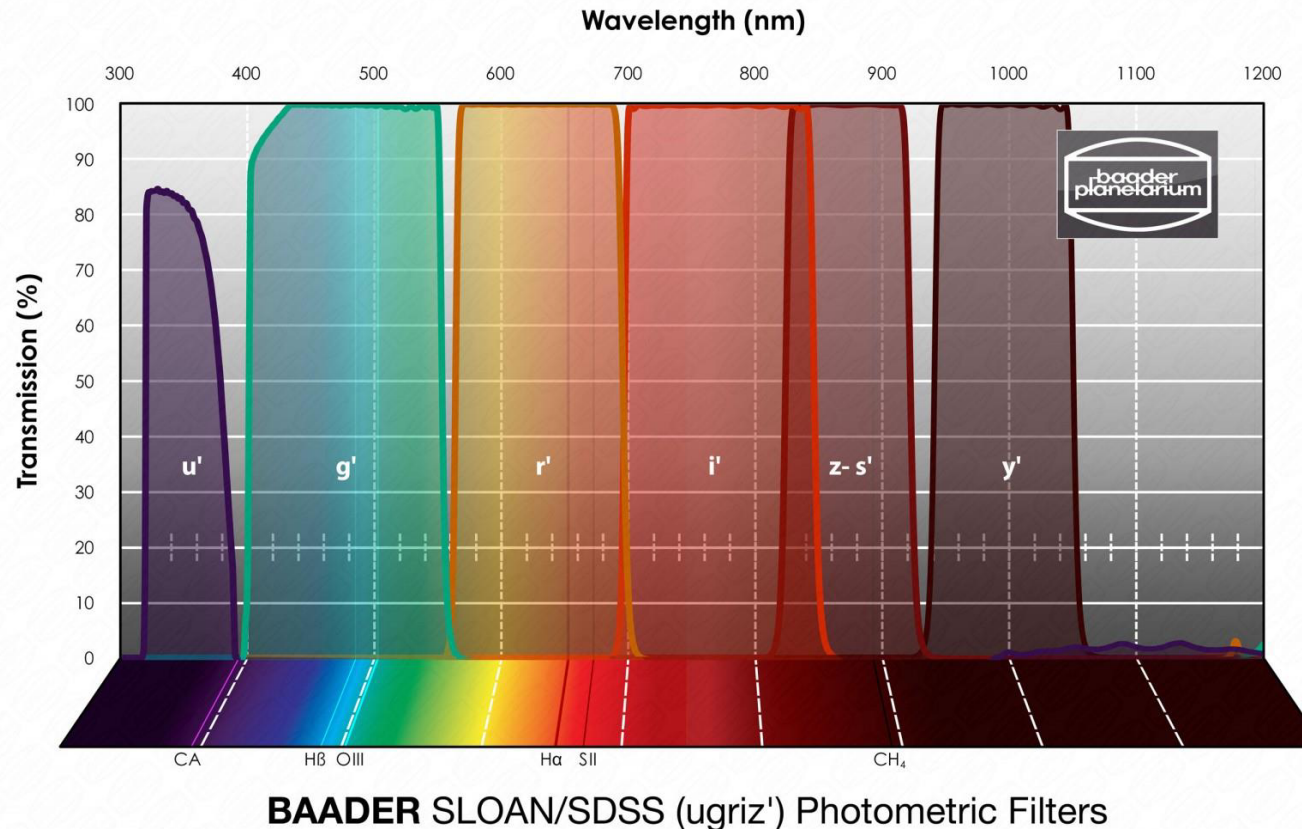
TOBi Telescopio Ottico Bicocca



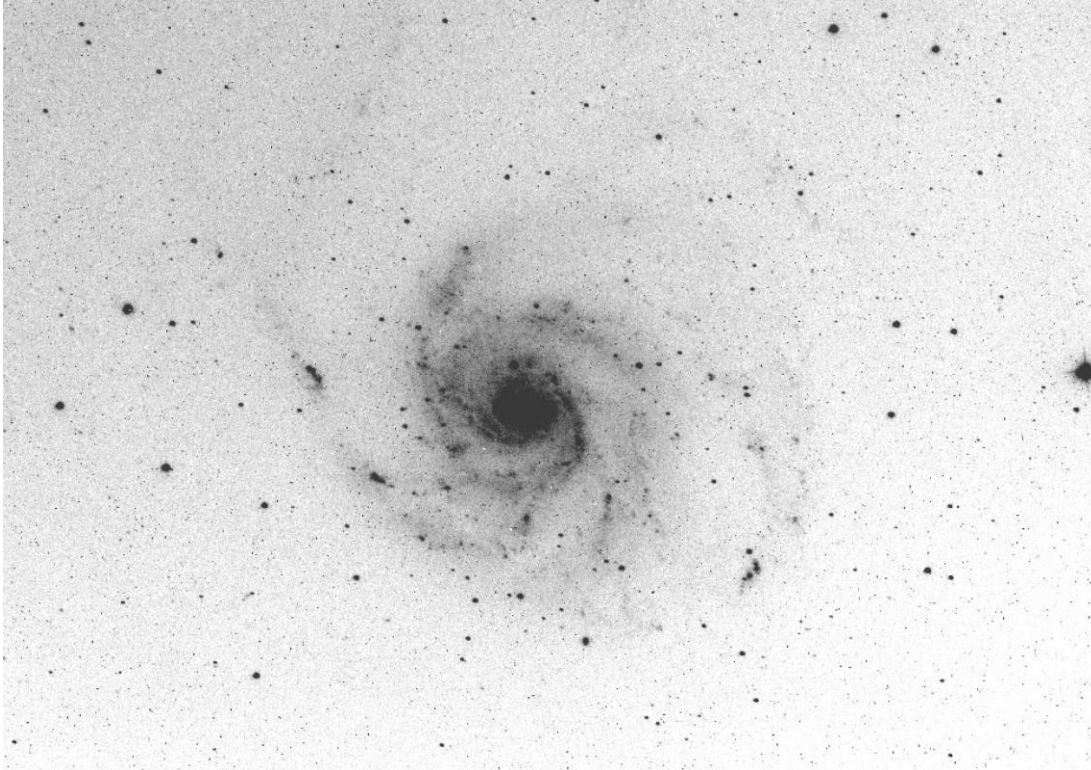
TOBi Telescopio Ottico Bicocca



TOBi Telescopio Ottico Bicocca



TOBi Telescopio Ottico Bicocca



M101 NGC 5457 $m(V)=8.3$

Some tens of seconds,
No filters
Just to verify alignment

Quite promising!

TOBi Telescopio Ottico Bicocca



M101 NGC 5457 $m(V)=8.3$

10 minutes per filter (r' , g' , i')

Supernova SN2023ixf still
shining after 2 month (image
shot on May 2023)!



TOBi Telescopio Ottico Bicocca

Spectrograph Starlight Express R~2000-3000

Self-collimating concave reflective grating spectrograph with a highly corrected flat field toroidal grating. Minimal attenuation of near UV, due to mostly reflecting optics.

Built-in Lodestar PRO Guide Camera and calibration source.

Grating specifications: **Groove pitch – 550 grooves per mm at centre of grating.** Blaze wavelength – 400 nm.

Spectral efficiency at 400 nm – Greater than 50%.

Useful spectral range – **340 to 900 nm**

Useful grating aperture – 26 x 26 mm.

Rotary slit wheel with 6 slit positions: Position 1 – 20 μm x 1 mm – Position 2 – 30 μm x 2 mm Position 3 – 55 μm x 2 mm – Position 4 – 115 μm x 2 mm Position 5 – 325 μm x 2 mm – Position 6 – 3mm x 3 mm circular

Size – 120 x 115 x 70 mm Weight – 1.17 kg



TOBi Telescopio Ottico Bicocca

Spectrograph Starlight Express R~2000-3000

Self-collimating concave reflective grating spectrograph with a highly corrected flat field toroidal grating. Minimal attenuation of near UV, due to mostly reflecting optics.

Built-in Lodestar PRO Guide Camera and calibration source.

Grating specifications: **Groove pitch – 550 grooves per mm at centre of grating.** Blaze wavelength – 400 nm.

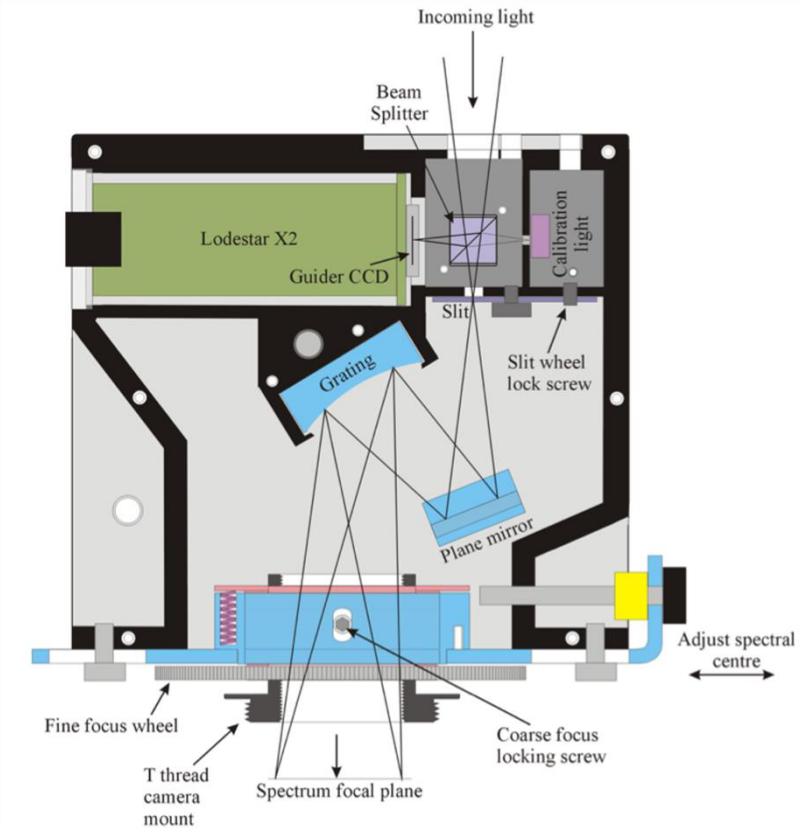
Spectral efficiency at 400 nm – Greater than 50%.

Useful spectral range – **340 to 900 nm**

Useful grating aperture – 26 x 26 mm.

Rotary slit wheel with 6 slit positions: Position 1 – 20 μm x 1 mm – Position 2 – 30 μm x 2 mm Position 3 – 55 μm x 2 mm – Position 4 – 115 μm x 2 mm Position 5 – 325 μm x 2 mm – Position 6 – 3mm x 3 mm circular

Size – 120 x 115 x 70 mm Weight – 1.17 kg



TOBi Telescopio Ottico Bicocca

On board computer is based on a win11 enterprise i5 4-core cpu

Everything is connected to EAGLE:

- dome
- mount
- Telescope
- Focuser
- Field Rotator
- Instruments

	EAGLE4 PRO
Processor:	Intel Core i5-8365U Quad core, Turbo 4,1 GHz
RAM memory: / SSD disk	16 GB / 480 GB
USB 3 ports:	3xUSB 3.1 type A 1xUSB 3.1 type C
USB 2 ports:	5xUSB 2.0
Thunderbolt 3:	<input checked="" type="checkbox"/>
Control via WiFi:	<input checked="" type="checkbox"/>
Control via Ethernet:	<input checked="" type="checkbox"/>
Remote ON/OFF power:	<input checked="" type="checkbox"/>
Remote ON/OFF USB ports:	<input checked="" type="checkbox"/> only four USB 2.0 ports
GPS sensor:	<input checked="" type="checkbox"/>
EYE sensor:	<input checked="" type="checkbox"/>
DARK mode:	<input checked="" type="checkbox"/>
Windows status LED:	<input checked="" type="checkbox"/>
Power out ports and max current:	7 12V ports , 4x12V + 3x0-12V
Max weight load capacity:	8 kg
Average power consumption:	1600 mA/hour
Operative system:	Windows 10 Enterprise



PLUS

TOBi Telescopio Ottico Bicocca

- Focuser ESATTO 4"
102mm aperture, 35mm travel, 0.04 μm res.
- Field Rotator ARCO 3"
76mm aperture, endless rotation, arc-sec res.



TOBi Telescopio Ottico Bicocca

- Scope Dome (PL) 3m V3
- Fully motorised and remotised (ARDUINO)
- Just fit for our telescope
- +/- 200° in azimuth
 - diameter of the dome: 3000 mm
 - shutter width: 1000 mm
 - dome height: 2400 mm
 - diameter of the base: 2760 mm
 - weight: ~330 kg



TOBi Telescopio Ottico Bicocca

CCD (Charged Coupled Device)

Solid State sensors (semiconductors) able to convert photons into electrons.

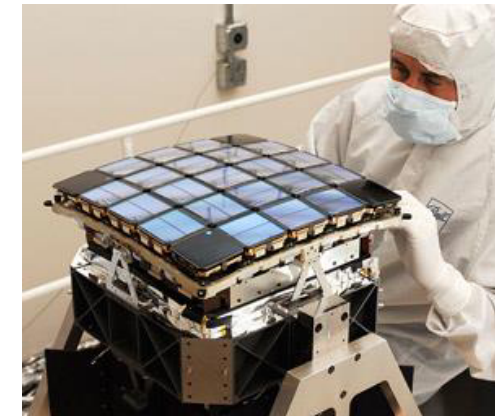
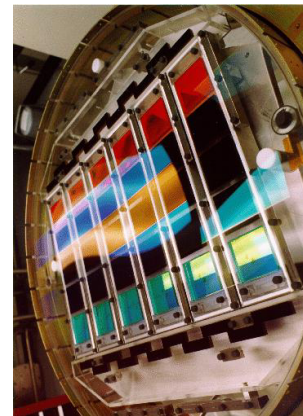
CCD haven't intrinsic energy (frequency) resolution in the visible domain.

Very high quantum efficiency (QE).

Mosaicing.

Based on the charge transfer principle

They are intrinsically monochrome



SDSS
30 CCD

Kepler mission
42 CCD

TOBi Telescopio Ottico Bicocca

Principle of operation: Photoelectric Effect (threshold)

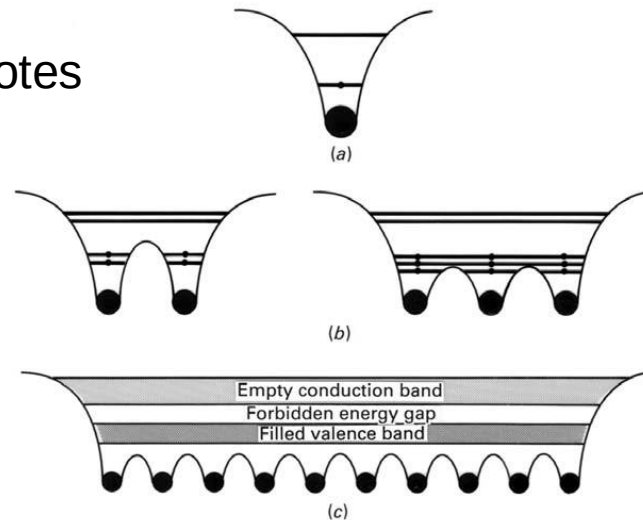
In semiconductors, a band structure takes place because of the lattice:

the absorption of a photon of sufficient energy promotes an electron from valence to conductive band

There is a cut-off wavelength above which the CCD is unsensitive:

$$\lambda_{co} = \frac{hc}{E_g} = \frac{1240 \text{ nm}}{E_g(\text{eV})}$$

In Silicon, $E_g=1.12 \text{ eV}$ so $\lambda_{co}=1100\text{nm}$



TOBi Telescopio Ottico Bicocca

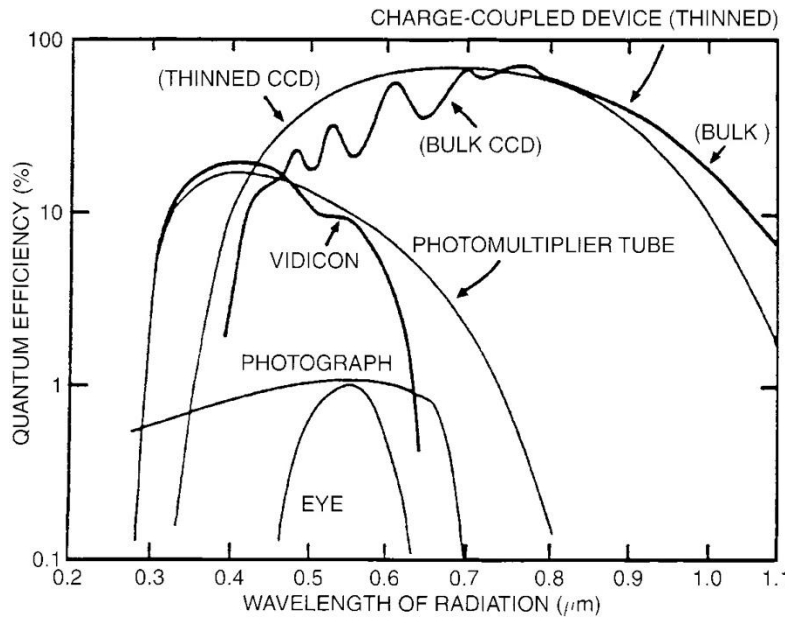


Fig. 3.2. QE curves for various devices, indicating why CCDs are a quantum leap above all previous imaging devices. The failure of CCDs at optical wavelengths shorter than about 3500 Å has been essentially eliminated via thinning or coating of the devices (see Figure 3.3).

In the visible domain CCDs are the most sensitive devices.

To extend their spectral coverage are

thinned and back-illuminated

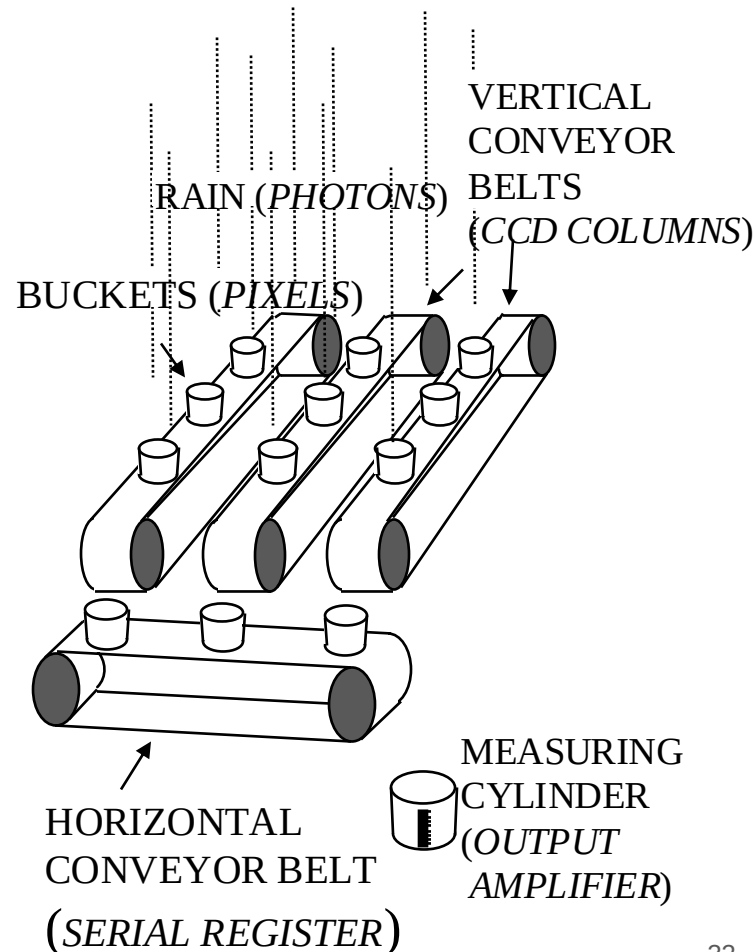
Detector type	QE	Special property
Photographic plates	2% (3% Kodak IIIaJ)	Sensitive to UV + blue light \Rightarrow need special coating to be sensible in visible.
Hypersensitized plates	10%	(chemically processed and cooled)
Electronic devices	20-40% bandpass similar to CCD	not precise in flux and position need high voltage to work
CCD	90%	reach $\sim 60\%$ over 2/3 of bandpass

TOBi Telescopio Ottico Bicocca

Principle of operation: Charge Transfer

- Once the exposure is terminated, the first row is transferred into the output serial register.
- The serial register transfer each charge in a charge preamplifier which converts the charge in a voltage signal
- When the serial register is empty, a new row is transferred and the readout process repeated

This can be done at high speed (MHz) letting a Mpix ccd to be read in fraction of a second (*readout noise, see later*)



TOBi Telescopio Ottico Bicocca

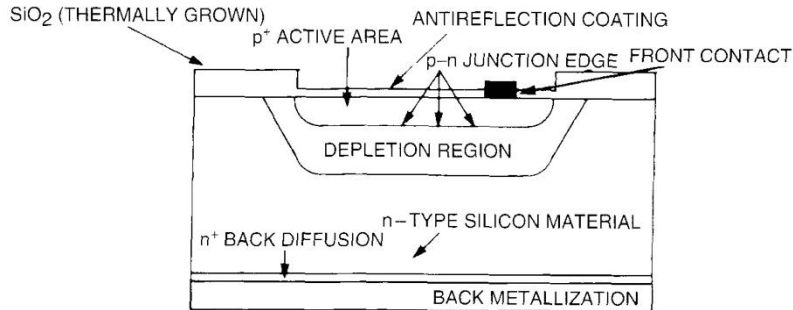
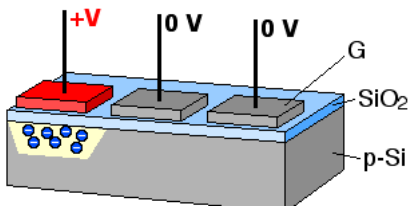


Fig. 2.4. Schematic view of a single front-side illuminated CCD pixel. The square labeled "front contact" is a representation of part of the overall gate structure. The letters "p" and "n" refer to regions within the pixel consisting of silicon doped with phosphorus and boron respectively.

Every pixel is a p-n junction reverse biased to obtain a depletion region where the electrons promoted from valence to conductive band are trapped since the exposure ends.



Changing the bias of the adjacent blind pixels translates in the pouring of the charge.

PROBLEM: electrodes reduce exposed area

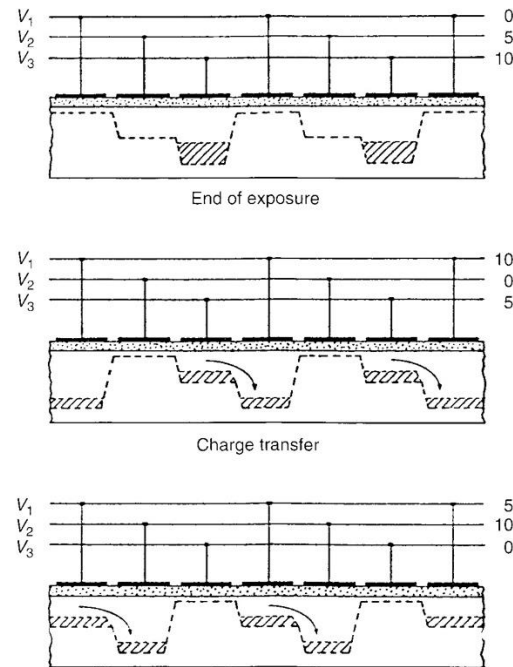
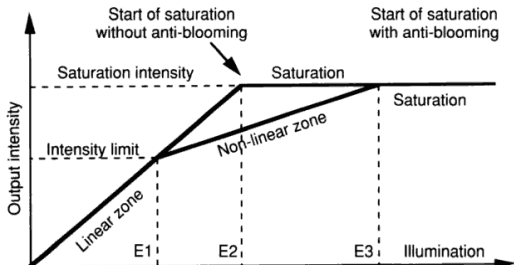
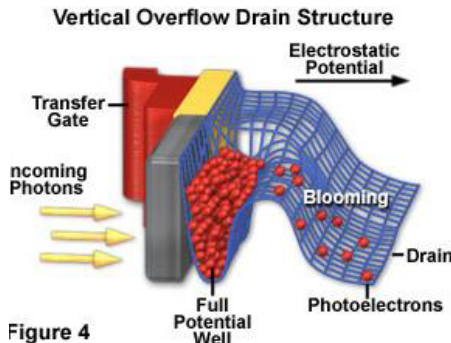


Fig. 2.2. Schematic voltage operation of a typical three-phase CCD. The clock voltages are shown at three times during the readout process, indicating their clock cycle of 0, 10, and 5 volts. One clock cycle causes the stored charge within a pixel to be transferred to its neighboring pixel. CCD readout continues until all the pixels have had their charge transferred completely out of the array and through the A/D converter. From Walker (1987).

TOBi Telescopio Ottico Bicocca



Blooming

Very bright sources can generate blooming effect when the well capacity is reached. The charge pours in the nearest vertical pixels creating stripes in the image.

Scientific CCDs do not employ anti-blooming architecture because it reduces the sensitive area and adds a non-linear zone before saturation.



In spectroscopic mode blooming can be used to enlarge dinamic range. Homework: how?

TOBi Telescopio Ottico Bicocca

CFH12K

Since neither the QE of a CCD nor the filter transmission are uniform, these data must be known to apply the color correction for an accurate photometry.

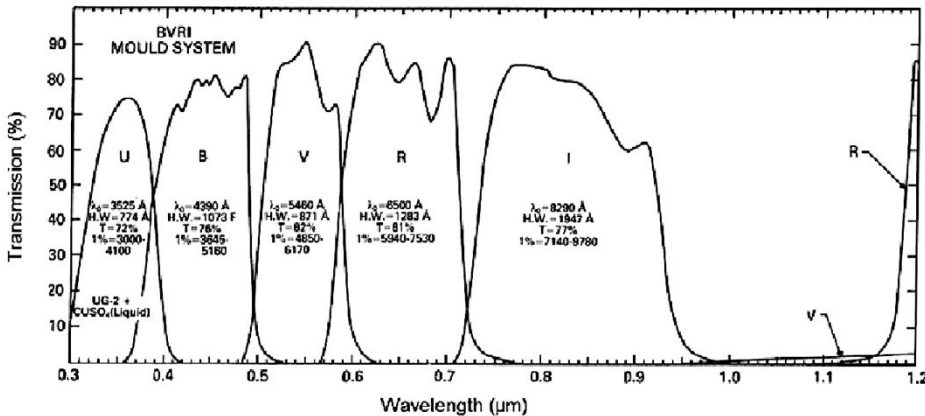
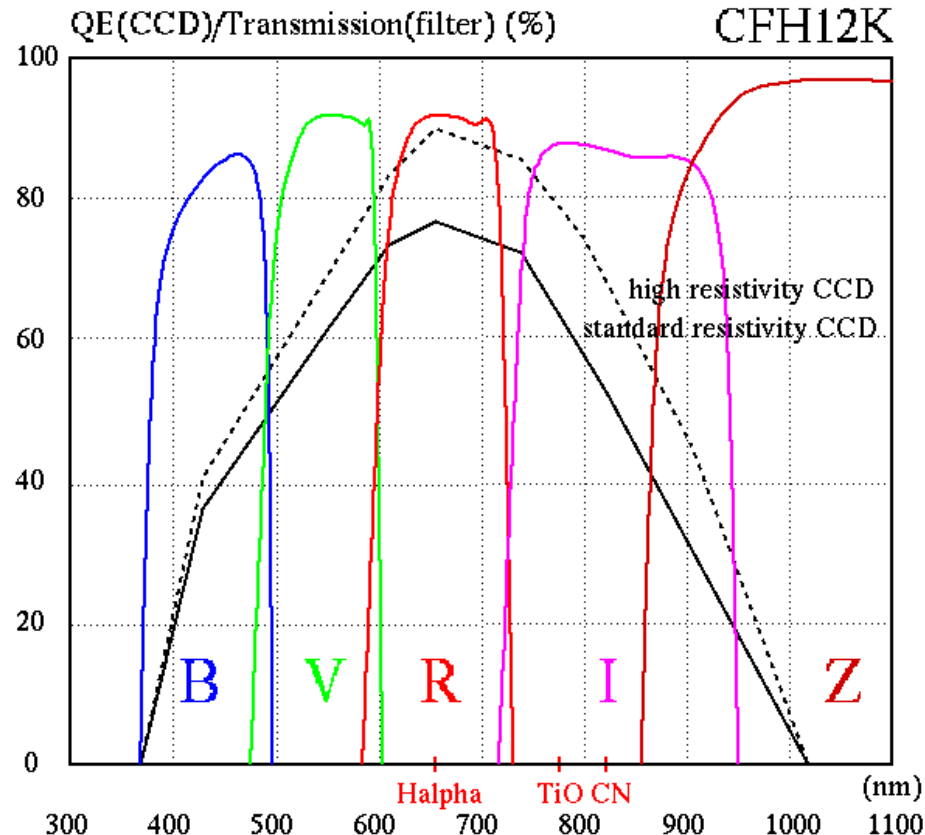


Figure 9.10. Standard filter bandpasses used with CCDs: the Mould system.



TOBi Telescopio Ottico Bicocca

If you use standard filters you can even be unaware of your DQE and use this table to calibrate your telescope-detector system.

Table 9.4. Absolute flux from a zero-magnitude star like Vega.

Symbol	λ (μm)	ν (Hz)	F_λ (W cm ⁻² μm ⁻¹)	F_ν (Jy)*
U	0.36	8.3×10^{14}	4.35×10^{-12}	1,880
B	0.43	7.0×10^{14}	7.20×10^{-12}	4,440
V	0.54	5.6×10^{14}	3.92×10^{-12}	3,810
R	0.70	4.3×10^{14}	1.76×10^{-12}	2,880
I	0.80	3.7×10^{14}	1.20×10^{-12}	2,500
J	1.25	2.4×10^{14}	2.90×10^{-13}	1,520
H	1.65	1.8×10^{14}	1.08×10^{-13}	980
K	2.2	1.36×10^{14}	3.8×10^{-14}	620
L	3.5	8.6×10^{13}	6.9×10^{-15}	280
M	4.8	6.3×10^{13}	2.0×10^{-15}	153
N	9.1	3.0×10^{13}	1.09×10^{-16}	37

* These units are called jansky. One jansky equals $10^{-26} \text{ W m}^{-2} \text{ Hz}^{-1}$, or $(3 \times 10^{-16}/\lambda^2) \text{ W cm}^{-2} \mu\text{m}^{-1}$ if λ is expressed in microns.

TOBi Telescopio Ottico Bicocca

DARK CURRENT

Strongly dependent on Temperature

It is due to the thermal jiggling which causes electron promotion from conduction to valence band

$$DC \approx e^{\alpha T} \text{ (thousands of } e^- \text{ per s at room } T\text{)}$$

DC typically doubles every $\Delta T = 5 - 10^\circ C$

Solution: cooling and stability

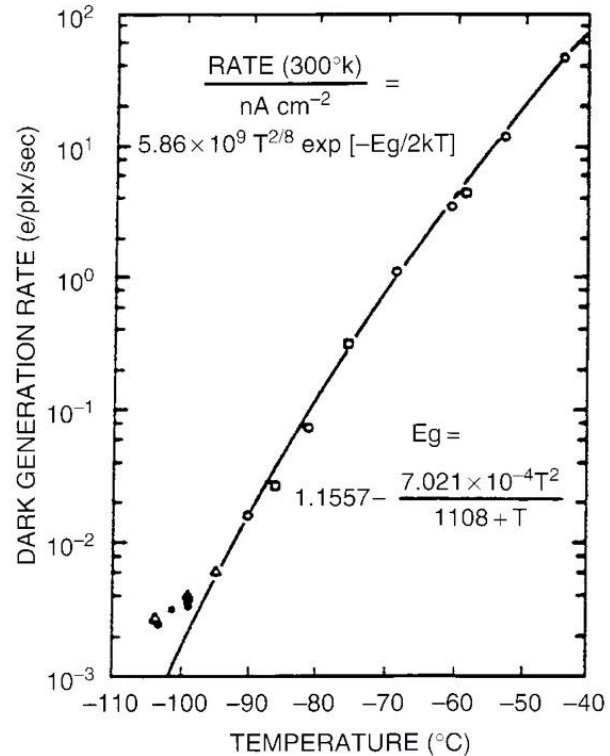


Fig. 3.6. Experimental (symbols) and theoretical (line) results for the dark current generated in a typical three-phase CCD. The rate of dark current, in electrons generated within each pixel every second, is shown as a function of the CCD operating temperature. E_g is the band gap energy for silicon. From Robinson (1988a).

TOBi Telescopio Ottico Bicocca

The LINEARITY of the full detection system (CCD+Charge preamplifier) is fundamental for an accurate photometry.

It depends on the pixel full well capacity and on the linearity of the Analogue to Digital Converter

Usually instrument data sheet provides this piece of information.

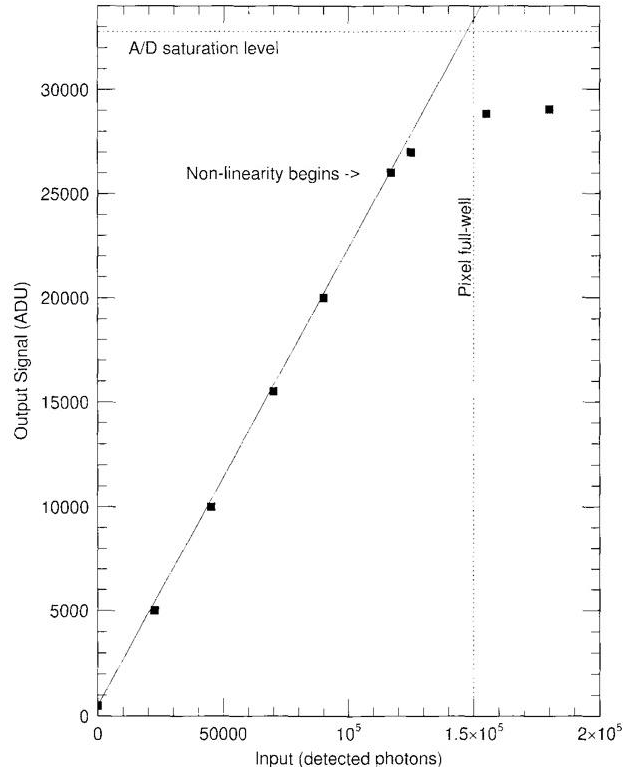


Fig. 3.9. CCD linearity curve for a typical three-phase CCD. We see that the device is linear over the output range from 500 ADU (the offset bias level of the CCD) to 26 000 ADU. The pixel full well capacity is 150 000 electrons and the A/D converter saturation is at 32 767 ADU. In this example, the CCD nonlinearity is the limiting factor of the largest usable output ADU value. The slope of the linearity curve is equal to the gain of the device.

TOBi Telescopio Ottico Bicocca

Detectors: CCD (Charge Coupled Devices)

CCD Equation

Based on *Poisson statistics*

$$\frac{S}{N} = \frac{N_*}{\sqrt{N_* + n_{pix}(N_B + N_D + N_R^2)}}$$

N_* = total # of photons (electrons) collected

n_{pix} = total # of pixels engaged

N_B = total # of background photons (electrons) per pixel

N_D = total # of dark “photons” (electrons) per pixel

N_R = total # of electrons per pixel due to readout noise

TOBi Telescopio Ottico Bicocca

CCD Equation

There is a more general version

$$\frac{S}{N} = \frac{N_*}{\sqrt{N_* + n_{pix} \left(1 + \frac{n_{pix}}{n_b}\right) (N_B + N_D + N_R^2 + G^2 \sigma_f^2)}}$$

N_* = total # of photons (electrons) collected

n_{pix} = total # of pixels engaged

N_B = total # of background photons (electrons) per pixel

N_D = total # of dark “photons” (electrons) per pixel

N_R = total # of electrons per pixel due to readout noise

n_b = total # of background pixel engaged

G = CCD gain

σ_f = estimate of the AD converter estra noise

Experimental Astronomy [0922-6435]

Merline, W J anno:**1995** vol:**6** fasc:**1-**

2 pag:163 -**210**

TOBi Telescopio Ottico Bicocca

We can make explicit the number of frames and the observing time per frame

$$SNR = \frac{S \cdot n_o \cdot t}{\sqrt{S \cdot n_o \cdot t + n_{pix}(B \cdot n_o \cdot t + Dark \cdot n_o \cdot t + n_o R^2)}} \quad n_o \text{ # of object frames}$$

2 asymptotic cases (we make explicit here the telescope diameter D)

1) Background-limited or sky limited case: $SNR \approx S\sqrt{t}[(n_{pix}B)]^{-1/2}$ since both S and $B \propto D^2$ $SNR \approx D$

2) Detector noise-limited case: $SNR \approx \frac{S \cdot n_o \cdot t}{\sqrt{n_{pix} \cdot n_o \cdot R^2}} = \frac{St}{R} \sqrt{\frac{n_o}{n_{pix}}} \approx D^2$

So, real advantage to go to giant telescope is for sources much fainter than the detector noise.

TOBi Telescopio Ottico Bicocca

$$\text{FINAL FRAME} = \frac{\text{OBJECT FRAME} - \text{BIAS(DARK) FRAME}}{\text{FLAT FRAME} - \text{BIAS(DARK) FRAME}}$$

BIAS FRAME

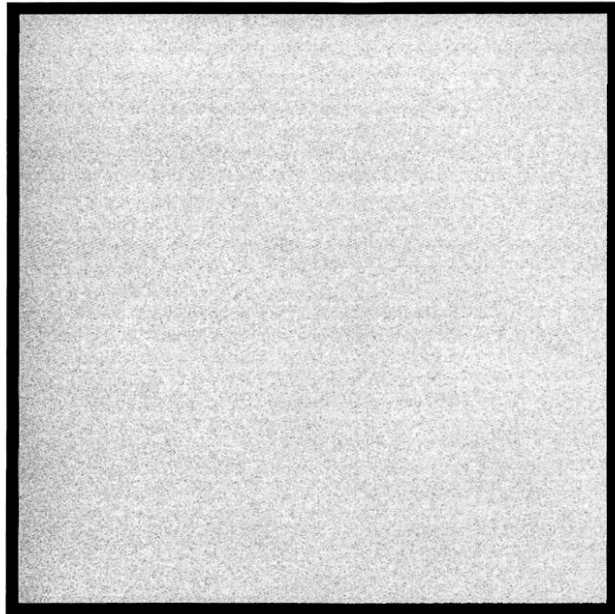


Fig. 4.2. Shown is a typical CCD bias frame. The histogram of this image was shown in Figure 3.8. Note the overall uniform structure of the bias frame.

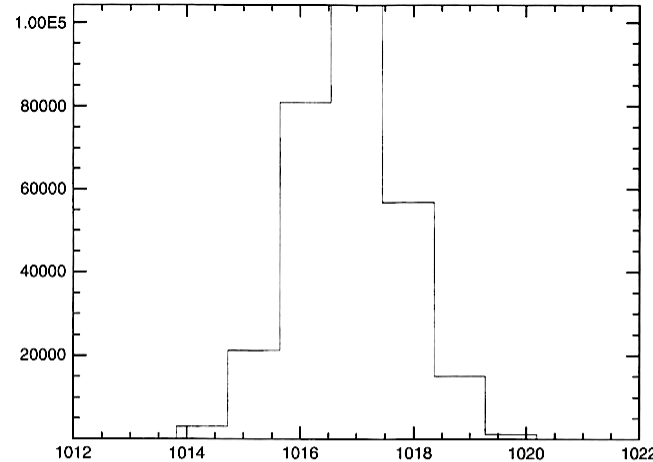
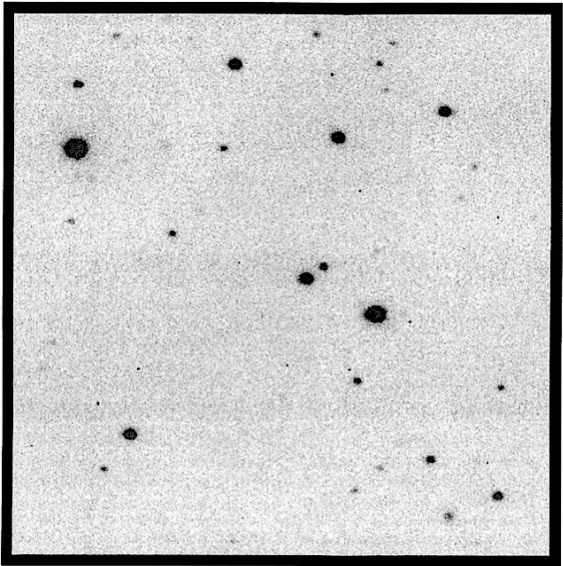


Fig. 3.8. Histogram of a typical bias frame showing the number of pixels vs. each pixel ADU value. The mean bias level offset or pedestal level in this Loral CCD is near 1017 ADU, and the distribution is very Gaussian in nature with a FWHM value of near 2 ADU. This CCD has a read noise of 10 electrons and a gain of $4.7 e^-/\text{ADU}$.

TOBi Telescopio Ottico Bicocca



OBJECT FRAME

$$\text{FINAL FRAME} = \frac{\text{OBJECT FRAME} - \text{BIAS(DARK) FRAME}}{\text{FLAT FRAME} - \text{BIAS(DARK) FRAME}}$$

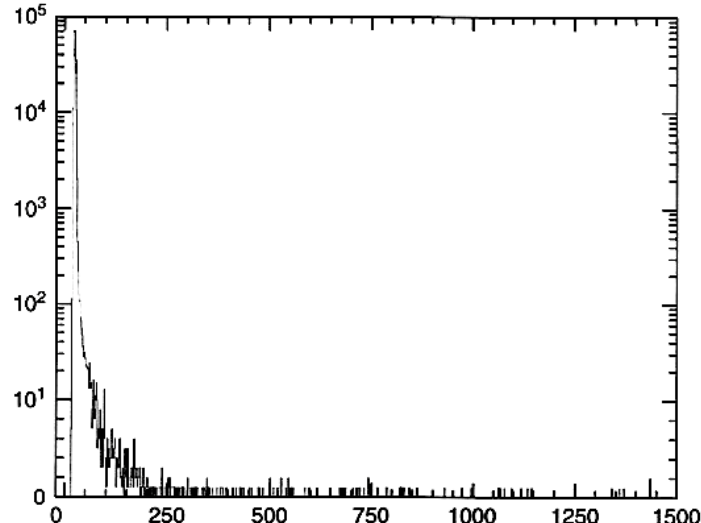
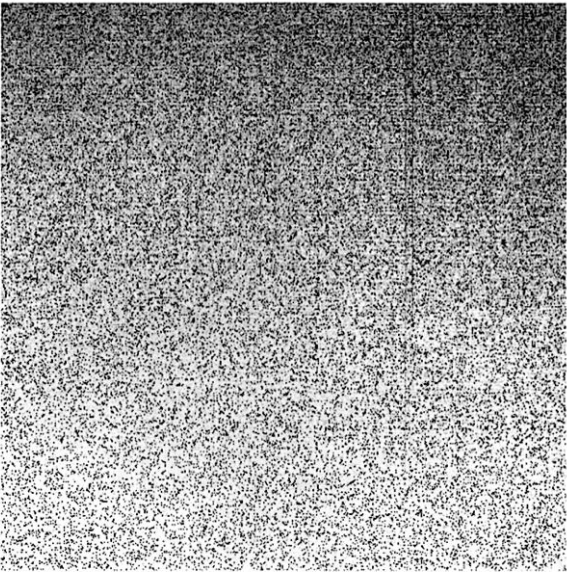


Fig. 4.5. (cont.)

Fig. 4.5. Shown is a typical CCD object frame showing a star field. This image has been properly reduced using bias frame subtraction and division by a flat field image. Note how the background is of a uniform level and distribution; all pixel-to-pixel nonuniformities have been removed in the reduction process. The stars are shown as black in this image and represent R magnitudes of 15th (brightest) to 20th (faintest). The histogram shown in the remainder of the figure is typical for a CCD object frame after reduction. The large grouping of output values on the left (values less than about 125 ADU) are an approximate Gaussian distribution of the background sky. The remaining histogram values (up to 1500 ADU) are the pixels that contain signal levels above the background (i.e., the pixels within the stars themselves!).

TOBi Telescopio Ottico Bicocca



DARK FRAME

Fig. 4.3. Shown is a typical CCD dark frame. This figure shows a dark frame for a Kodak CCD operating in MPP mode and thermoelectrically cooled. Notice the nonuniform dark level across the CCD, being darker (greater ADU values) on the top. Also notice the two prominent partial columns with higher dark counts, which extend from the top toward the middle of the CCD frame. These are likely to be column defects in the CCD that occurred during manufacture, but with proper dark subtraction they are of little consequence. The continuation of the figure shows the histogram of the dark frame. Most of the dark current in this 180 second exposure is uniformly distributed near a mean value of 180 ADU with a secondary maximum near 350 ADU. The secondary maximum represents a small number of CCD pixels that have nearly twice the dark current of the rest, again most likely due to defects in the silicon lattice. As long as these increased dark current pixels remain constant, they are easily removed during image calibration.

$$\text{FINAL FRAME} = \frac{\text{OBJECT FRAME} - \text{BIAS(DARK) FRAME}}{\text{FLAT FRAME} - \text{BIAS(DARK) FRAME}}$$

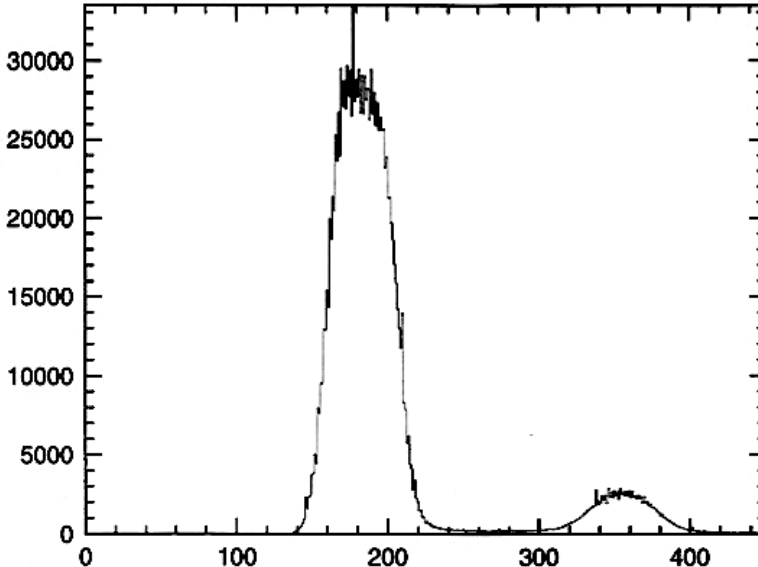
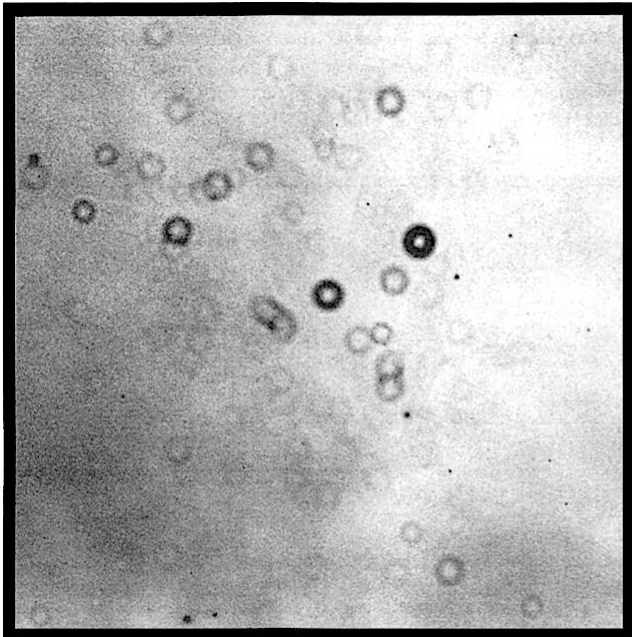


Fig. 4.3. (cont.)

TOBi Telescopio Ottico Bicocca



FLAT FIELD
FRAME

$$\text{FINAL FRAME} = \frac{\text{OBJECT FRAME} - \text{BIAS(DARK) FRAME}}{\text{FLAT FRAME} - \text{BIAS(DARK) FRAME}}$$

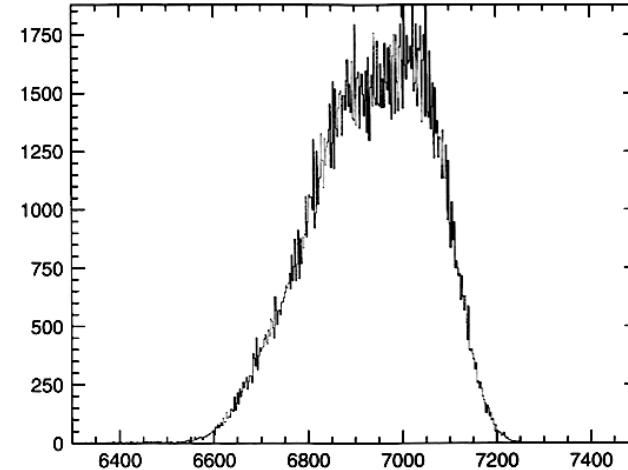


Fig. 4.1. Histogram of a typical flat field image. Note the fairly Gaussian shape of the histogram and the slight tail extending to lower values. For this R-band image, the filter and dewar window were extremely dusty leading to numerous out of focus "doughnuts" (see Figure 4.4), each producing lower than average data values.

Fig. 4.4. Shown is a typical CCD flat field image. This is an R-band flat field image for a 1024×1024 Loral CCD. The numerous "doughnuts" are out of focus dust specks present on the dewar window and the filter. The varying brightness level and structures are common in flat field images. As seen in the histogram of this image (Figure 4.1) this flat field has a mean level near 6950 ADU, with an approximate dispersion (FWHM) 400 ADU.